

## **New Insights into Li Distribution in the Superionic Argyrodite**

### **Li<sub>6</sub>PS<sub>5</sub>Cl**

Enyue Zhao<sup>a,b</sup>, Lunhua He<sup>b,c</sup>, Zhigang Zhang<sup>b</sup>, Jean-Marie Doux<sup>a</sup>, Darren H. S. Tan<sup>a</sup>, Erik A. Wu<sup>a</sup>,  
Grayson Deysher<sup>d</sup>, YuTing Chen<sup>d</sup>, Jinkui Zhao<sup>b</sup>, Fangwei Wang<sup>b,c</sup>, Ying Shirley Meng<sup>\*a,d,e</sup>

<sup>a</sup> Department of NanoEngineering, University of California, San Diego, La Jolla, CA 92093, United States

<sup>b</sup> Songshan Lake Materials Laboratory, Dongguan 523808, PR China

<sup>c</sup> Spallation Neutron Source Science Center, Dongguan, 523803, PR China

<sup>d</sup> Program of Materials Science and Engineering, University of California, San Diego, La Jolla, CA 92093, United States

<sup>e</sup> Sustainable Power & Energy Center (SPEC), University of California San Diego, La Jolla, CA 92093, United States

\* shirleymeng@ucsd.edu

## Experimental Section

Li<sub>6</sub>PS<sub>5</sub>Cl powder was purchased from NEI Corporation (USA). X-ray diffraction (XRD) patterns were obtained by sealing the powders in boron-rich glass capillaries in an Ar-filled glovebox. Measurements were taken using Cu K $\alpha$  radiation in a Bruker/Nonius Microstar 592 diffractometer. Scanning electron microscope (SEM) images of the Li<sub>6</sub>PS<sub>5</sub>Cl powder were obtained with a FEI Scios DualBeam Focused ion beam. The sample was prepared in an Ar-filled glovebox and transferred with an air-tight loader to avoid any atmosphere exposure. Variable temperature (5 K, 300 K, and 550 K) neutron powder diffraction (NPD) data was collected at the beamline of the General Purpose Powder Diffractometer (GPPD) at the China Spallation Neutron Source (CSNS). Rietveld refinements and maximum entropy method (MEM) analysis were carried out using the FullProf Suite software package<sup>1</sup> and Dysnomia software<sup>2</sup>, respectively.

For the Rietveld refinements analysis of NPD data, the peak profile shape was described by the function of T.O.F. p-Voigt \* B-t-B exponential. During the refinement, the fit indicators  $R_{wp}$  was used to assess the quality of the refined structural model. The following parameters were initially refined: (1) scale factor, (2) background (Linear Interpolation between a set background points with refinable heights), (3) shape parameters, and (4) cell parameters. After a suitable fit of the profile was achieved, the structural parameters, including 5) fractional atomic coordinates, (6) isotropic atomic displacement parameters, and (7) atomic occupancies, were then refined. The output atomic displacement parameters ( $U_{iso}$ ) were used as indicators for exploring the authenticity of the eventual occupancy. In order to ensure the stability of the refinements, multiple correlated parameters were simultaneously refined over several cycles. The refinement analysis for the various-temperature NPD data were performed in a sequential mode and the consistency of the obtained structural models was corroborated by introducing different starting parameters. Constraints used for the refinement analysis of NPD data are shown in Table S2.

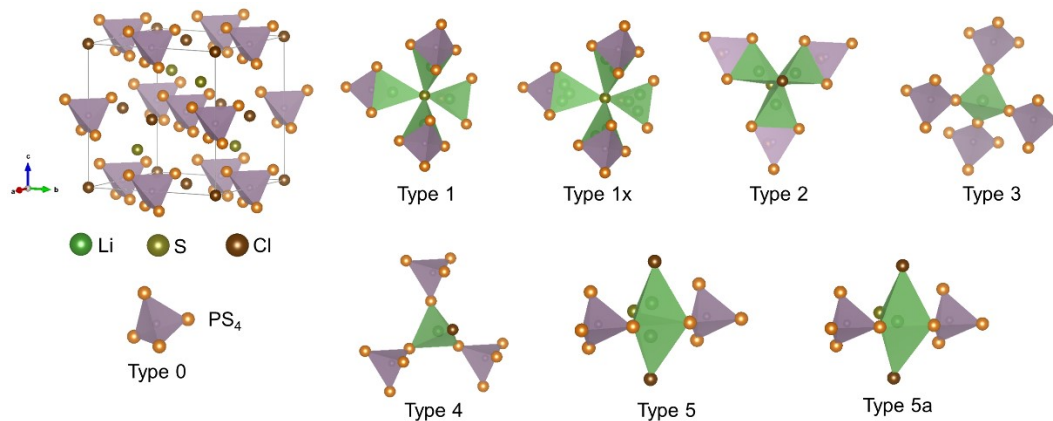


**Fig. S1** Crystal structure of the lithium argyrodites  $\text{Li}_6\text{PS}_5\text{X}$  ( $X = \text{Cl, Br, I}$ ), with panels showing the typical local coordination of the six types of tetrahedral interstitial sites (type 0-5), alongside the trigonally-coordinated type 5a site and tetrahedrally-coordinated type 1x site.

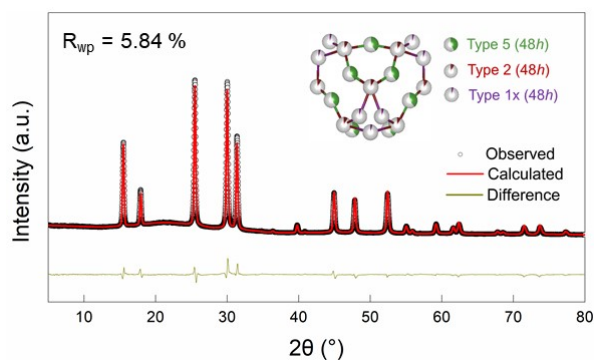


**Fig. S2** XRD data of  $\text{Li}_6\text{PS}_5\text{Cl}$  compound collected at room temperature and Rietveld refinement results based on the Li sublattice structure model (inset) with type 5, type 2 and type 1x Li positions.

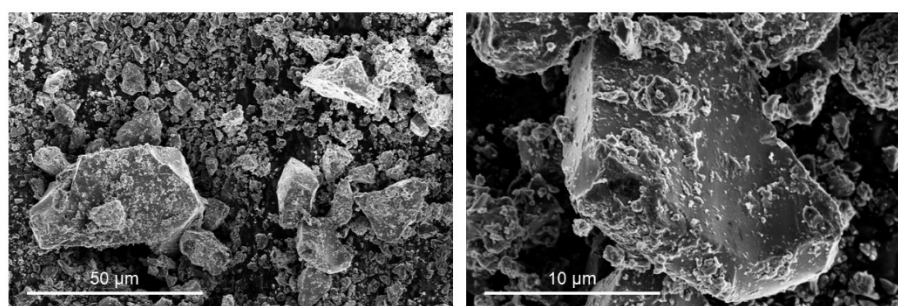


**Fig. S3** SEM results of  $\text{Li}_6\text{PS}_5\text{Cl}$  powder. It can be seen that the  $\text{Li}_6\text{PS}_5\text{Cl}$  particles have irregular shape and the particle size is on the micron scale.

**Table S1** Neutron coherent scattering lengths and coherent, incoherent, and absorption cross-sections of Li, P, S and Cl in Li<sub>6</sub>PS<sub>5</sub>Cl (as obtained from <https://www.ncnr.nist.gov/resources/neutron-lengths/>).

Element	Coh b (fm)	Coh xs (barn)	Inc xs (barn)	Abs xs (barn)
Li	-1.90	0.454	0.92	70.5
P	5.13	3.307	0.005	0.172
S	2.847	1.0186	0.007	0.53
Cl	9.5770	11.5257	5.3	33.5

**Table S2** Constraints used for the refinement analysis of neutron powder diffraction data of the Li<sub>6</sub>PS<sub>5</sub>Cl compound.

Atom	Site	x	y	z	Occ.	U <sub>iso</sub> (Å <sup>2</sup> )
P1	4b	0	0	0.5	1	<i>Variation1</i>
Cl1	4a	0	0	1	<i>Occ1</i>	<i>Variation2</i>
Cl2	4d	0.25	0.25	0.75	1- <i>Occ1</i>	<i>Variation3</i>
Li <sub>type5</sub>	48h	<i>Site1</i>	<i>Site2</i>	1- <i>Site1</i>	<i>Occ2</i>	<i>Variation4</i>
Li <sub>type2</sub>	48h	0.25	<i>Site3</i>	0.5+ <i>Site3</i>	<i>Occ3</i>	<i>Variation5</i>
Li <sub>type1x</sub>	48h	<i>Site4</i>	<i>Site4</i>	<i>Site5</i>	<i>Occ4</i>	<i>Variation6</i>
Li <sub>type5a</sub>	24g	0.25	<i>Site6</i>	0.75	<i>Occ5</i>	<i>Variation7</i>
S1	4d	0.25	0.25	0.75	<i>Occ1</i>	<i>Variation3</i>
S2	16e	<i>Site7</i>	- <i>Site7</i>	0.5+ <i>Site7</i>	1	<i>Variation8</i>
S3	4a	0	0	1	1- <i>Occ1</i>	<i>Variation2</i>

Note:  $Occ2 + Occ3 + Occ4 + 1/2Occ5 = 0.5$

**Table S3** The refined crystal structure of Li<sub>6</sub>PS<sub>5</sub>Cl using neutron powder diffraction data collected at 5 K (in this case, only the type 5 Li Wyckoff site was considered in the refinement structure model).

S.G. F -4 3 m, a = 9.79657(7) Å R <sub>wp</sub> = 2.56 %
--

Atom	Site	x	y	z	Occ.	$U_{\text{iso}} (\text{\AA}^2)$
P1	4 <i>b</i>	0	0	0.5	1	0.0210(13)
Cl1	4 <i>a</i>	0	0	1.0	0.447(7)	0.0164(16)
Cl2	4 <i>d</i>	0.25	0.25	0.75	0.553(7)	0.0198(13)
Li <sub>type5</sub>	48 <i>h</i>	0.3170(4)	0.0228(5)	0.6831(4)	0.500(7)	0.0482(19)
S1	4 <i>d</i>	0.25	0.25	0.75	0.447(7)	0.0198(13)
S2	16 <i>e</i>	0.1189(2)	-0.1189(2)	0.6189(2)	1	0.0280(10)
S3	4 <i>a</i>	0	0	1.0	0.553(7)	0.0164(16)

**Table S4** The refined crystal structure of Li<sub>6</sub>PS<sub>5</sub>Cl using neutron powder diffraction data collected at 5 K (in this case, only the type 5 and type 2 Li Wyckoff sites were considered in the refinement structure model).

S.G. F -4 3 m, a = 9.79657(6) Å $R_{\text{wp}} = 2.26 \%$						
Atom	Site	x	y	z	Occ.	$U_{\text{iso}} (\text{\AA}^2)$
P1	4 <i>b</i>	0	0	0.5	1	0.0194(10)
Cl1	4 <i>a</i>	0	0	1	0.483(7)	0.0274(15)
Cl2	4 <i>d</i>	0.25	0.25	0.75	0.517(7)	0.0182(10)
Li <sub>type5</sub>	48 <i>h</i>	0.3207(6)	0.0244(6)	0.6794(6)	0.415(6)	0.042(2)
Li <sub>type2</sub>	48 <i>h</i>	0.25	0.4474(14)	0.9474(14)	0.085(6)	0.011(8)
S1	4 <i>d</i>	0.25	0.25	0.75	0.483(7)	0.0182(10)
S2	16 <i>e</i>	0.1189(2)	-0.1189(2)	0.6189(2)	1	0.0279(9)
S3	4 <i>a</i>	0	0	1	0.517(7)	0.0274(15)

**Table S5** The refined crystal structure of Li<sub>6</sub>PS<sub>5</sub>Cl using neutron powder diffraction data collected at 300 K (in this case, only the type 5 Li Wyckoff site was considered in the refinement structure model).

S.G. F -4 3 m, a = 9.83664(7) Å $R_{\text{wp}} = 2.20 \%$						
Atom	Site	x	y	z	Occ.	$U_{\text{iso}} (\text{\AA}^2)$
P1	4 <i>b</i>	0	0	0.5	1	0.0259(11)

Cl1	4a	0	0	1	0.460(8)	0.0266(18)
Cl2	4d	0.25	0.25	0.75	0.540(8)	0.0279(13)
Li <sub>type5</sub>	48h	0.3145(4)	0.0268(6)	0.6856(4)	0.500(8)	0.078(3)
S1	4d	0.25	0.25	0.75	0.460(8)	0.0279(13)
S2	16e	0.1194(3)	-0.1194(3)	0.6194(3)	1	0.0368(8)
S3	4a	0	0	1	0.540(8)	0.0266(18)

**Table S6** The refined crystal structure of Li<sub>6</sub>PS<sub>5</sub>Cl using neutron powder diffraction data collected at 300 K (in this case, type 5 and type 2 Li Wyckoff sites were considered in the refinement structure model).

S.G. F -4 3 m, a = 9.83667(6) Å R <sub>wp</sub> = 1.95 %						
Atom	Site	x	y	z	Occ.	U <sub>iso</sub> (Å <sup>2</sup> )
P1	4b	0	0	0.5	1	0.0216(9)
Cl1	4a	0	0	1.0	0.501(8)	0.0354(16)
Cl2	4d	0.25	0.25	0.75	0.499(8)	0.0231(12)
Li <sub>type5</sub>	48h	0.3182(8)	0.0302(8)	0.6819(8)	0.413(7)	0.081(4)
Li <sub>type2</sub>	48h	0.25	0.4458(15)	0.9458(15)	0.087(7)	0.019(11)
S1	4d	0.25	0.25	0.75	0.501(8)	0.0231(12)
S2	16e	0.1199(3)	-0.1199(3)	0.6199(3)	1	0.0342(7)
S3	4a	0	0	1.0	0.499(8)	0.0354(16)

**Table S7** The refined crystal structure of Li<sub>6</sub>PS<sub>5</sub>Cl using neutron powder diffraction data collected at 300 K (in this case, type 5, type 2 and type 1x Li Wyckoff sites were considered in the refinement structure model).

S.G. F -4 3 m, a = 9.83665(6) Å R <sub>wp</sub> = 1.91 %						
Atom	Site	x	y	z	Occ.	U <sub>iso</sub> (Å <sup>2</sup> )
P1	4b	0	0	0.5	1	0.0245(9)
Cl1	4a	0	0	1	0.481(8)	0.0321(17)
Cl2	4d	0.25	0.25	0.75	0.518(8)	0.0254(12)

Li <sub>type5</sub>	48h	0.3181(7)	0.0289(7)	0.6820(7)	0.387(8)	0.061(3)
Li <sub>type2</sub>	48h	0.25	0.4468(15)	0.9468(15)	0.079(4)	0.014(8)
Li <sub>type1x</sub>	48h	0.59776 <sup>^</sup>	0.59776 <sup>^</sup>	0.515(6)	0.034(4)	0.01297 <sup>^</sup>
S1	4d	0.25	0.25	0.75	0.481(8)	0.0254(12)
S2	16e	0.1194(3)	-0.1194(3)	0.6195(3)	1	0.0357(7)
S3	4a	0	0	1	0.518(8)	0.0321(17)

<sup>^</sup> = initially refined then fixed

**Table S8** The refined crystal structure of Li<sub>6</sub>PS<sub>5</sub>Cl using neutron powder diffraction data collected at 550 K (in this case, type 5, type 2 and type 1x Li Wyckoff sites were considered in the refinement structure model).

S.G. F -4 3 m, a = 9.90337(8) Å R <sub>wp</sub> = 2.05 %						
Atom	Site	x	y	z	Occ.	U <sub>iso</sub> (Å <sup>2</sup> )
P1	4b	0	0	0.5	1	0.0323(17)
Cl1	4a	0	0	1.0	0.448(11)	0.035(2)
Cl2	4d	0.25	0.25	0.75	0.552(11)	0.039(2)
Li <sub>type5</sub>	48h	0.3119(8)	0.0283(9)	0.6882(8)	0.343(11)	0.038(3)
Li <sub>type2</sub>	48h	0.25	0.441(3)	0.941(3)	0.073(5)	0.039(8)
Li <sub>type1x</sub>	48h	0.59317 <sup>^</sup>	0.59317 <sup>^</sup>	0.515(3)	0.084(5)	0.01297 <sup>^</sup>
S1	4d	0.25	0.25	0.75	0.448(11)	0.039(2)
S2	16e	0.1177(3)	-0.1177(3)	0.6177(3)	1	0.0455(16)
S3	4a	0	0	1.0	0.552(11)	0.035(2)

<sup>^</sup> = initially refined then fixed

**Table S9** The refined crystal structure of Li<sub>6</sub>PS<sub>5</sub>Cl using neutron powder diffraction data collected at 550 K (in this case, type 5, type 2, type 1x and type 5a Li Wyckoff sites were considered in the refinement structure model).

S.G. F -4 3 m, a = 9.90336(8) Å R <sub>wp</sub> = 2.01 %						
Atom	Site	x	y	z	Occ.	U <sub>iso</sub> (Å <sup>2</sup> )
P1	4b	0	0	0.5	1	0.0313(17)

Cl1	4a	0	0	1	0.489(12)	0.049(3)
Cl2	4d	0.25	0.25	0.75	0.510(12)	0.0376(19)
Li <sub>type5</sub>	48h	0.3163(11)	0.0322(12)	0.6838(11)	0.334(12)	0.072(4)
Li <sub>type2</sub>	48h	0.25	0.4430(18)	0.9430(18)	0.094(8)	0.027(11)
Li <sub>type1x</sub>	48h	0.59317 <sup>^</sup>	0.59317 <sup>^</sup>	0.516(5)	0.058(8)	0.01297 <sup>^</sup>
Li <sub>type5a</sub>	24g	0.25	0.00922 <sup>^</sup>	0.75	0.029(8)	0.01193 <sup>^</sup>
S1	4d	0.25	0.25	0.75	0.489(12)	0.0376(19)
S2	16e	0.1185(3)	-0.1185(3)	0.6186(3)	1	0.0454(18)
S3	4a	0	0	1	0.510(12)	0.049(3)

<sup>^</sup> = initially refined then fixed

**Table S10** Concentration of Li ions in the argyrodite lattice based on the refinement results of the temperature-dependent neutron powder diffraction data.

	5 K	300 K	550 K
Type 5	~ 83.0%	~ 77.4%	~ 66.7%
Type 2	~ 17.0%	~ 15.8%	~ 18.8%
Type 1x	0	~ 6.8%	~ 11.6%
Type 5a	0	0	~ 2.9%

**Table S11** The summarized bond valence sums (BVS) for Li sites at various temperatures.

Li sites	5 K	300 K	550 K
Type 5	0.93	0.91	0.87
Type 2	1.26	1.21	1.41
Type 1x	--	1.18	0.91
Type 5a	--	--	1.19

**Table S12** Summary of the Li-S, Li-Cl and Li-Li bond lengths at various temperatures, which are observed from the refinement results of the neutron diffraction data.

	5 K	300 K	550 K
--	-----	-------	-------



Li <sub>T5</sub> -S <sub>16e</sub> (Å)	2.496	2.515	2.545
Li <sub>T5</sub> -Cl/S <sub>4d</sub> (Å)	2.417	2.372	2.348
Li <sub>T5</sub> -Cl/S <sub>4a</sub> (Å)	2.496	2.547	2.593
Li <sub>T5</sub> -Li <sub>T5</sub> (Å)	2.147	2.129	2.12
Li <sub>T2</sub> -S <sub>16e</sub> (Å)	2.212	2.227	2.256
Li <sub>T2</sub> -Cl/S <sub>4d</sub> (Å)	2.735	2.738	2.703
Li <sub>T2</sub> -Cl/S <sub>4a</sub> (Å)	2.555	2.568	2.601
Li <sub>T2</sub> -Li <sub>T2</sub> (Å)	2.73	2.74	2.70
Li <sub>T1x</sub> -S <sub>16e</sub> (Å)	--	2.38	2.34
Li <sub>T1x</sub> -Cl/S <sub>4d</sub> (Å)	--	3.14	3.19
Li <sub>T1x</sub> -Li <sub>T1x</sub> (Å)	--	1.15	1.08
Li <sub>T5a</sub> -S <sub>16e</sub> (Å)	--	--	2.234
Li <sub>T5a</sub> -Cl/S <sub>4d</sub> (Å)	--	--	2.385
Li <sub>T5a</sub> -Li <sub>T5</sub> (Å)	--	--	3.372

**Table S13** Coordinates of all possible Li sites in the Li<sub>6</sub>PS<sub>5</sub>Cl lattice structure utilized as starting point for the refinements<sup>3</sup>.

Li sites	Wyckoff Site	x	y	z
Type 1	16e	0.9	0.9	0.6
Type 1x	48h	0.59	0.59	0.51
Type 2	48h	0.25	0.433	0.933
Type 3	4c	0.25	0.25	0.25
Type 4	16e	0.15	0.15	0.15
Type 5	48h	0.304	0.025	0.695
Type 5a	24g	0.25	0.009	0.75

Notes: The possible type 1, type 3 as well as type 4 Li positions were tried during the refinement of various-temperature neutron powder diffraction data. The resulted preferred unphysical/negative values of atomic displacement parameters (Uiso) during the refinement indicated that these Li sites are not populated within the compositions and temperature range probed here. These results are moreover consistent with those from literature<sup>3</sup>.

## References

- 1 Rodriguez-Carvajal, J., *Physica B.*, 1993, **192**, 55.
- 2 K. Momma, T. Ikeda, A. A. Belik and F. Izumi, *Powder Diffraction*, 2013, **28**, 184-193.
- 3 N. Minafra, M. A. Kraft, T. Bernges, C. Li, R. Schlem, B. J. Morgan and W. G. Zeier, *Inorg. Chem.*, 2020, 59, 11009-11019.